JOURNAL OF CATALYSIS 112, 543–555 (1988)

Effects of Cerium Addition on CO Oxidation Kinetics over Alumina-Supported Rhodium Catalysts

SE H. OH AND CAROLYN C. EICKEL

Physical Chemistry Department, General Motors Research Laboratories, Warren, Michigan 48090-9055

Received November 12, 1987; revised March 7, 1988

The kinetics of CO oxidation in a strongly oxidizing environment (i.e., $P_{O_2} \gg P_{CO}$) over a low-loaded Rh/Al_2O_3 catalyst are not significantly affected by the presence of cerium. Under moderately oxidizing or net-reducing conditions, on the other hand, the addition of sufficient amounts of cerum oxides (≥2 wt% Ce) to the Rh/Al_2O_3 catalyst was found to cause the following changes in CO oxidation kinetics: suppression of the CO inhibition effect, decreased sensitivity of the reaction rate to gas-phase O_2 concentration, and decreased apparent activation energy. These cerium-induced changes in the kinetics lead to enhancement of CO oxidation activity and can be rationalized on the basis of a mechanism involving CO_2 formation via a reaction between CO adsorbed on Rh and surface oxygen derived from the neighboring ceria particles. The effects of Ce addition on the CO oxidation kinetics were also independent of whether the Ce was deposited before or after the Rh.

INTRODUCTION

Cerium oxide is a major base metal additive for commercial three-way catalysts used for the simultaneous conversion of carbon monoxide, hydrocarbons, and nitrogen oxides in automobile exhaust. The operating environment of three-way catalysts is characterized by oscillations in the feedstream composition between net-oxidizing and net-reducing conditions, and Ce is generally added to automotive catalysts to promote the water–gas shift reaction and to store oxygen in this oscillating environment (*1–3*). It has also been claimed that Ce stabilizes the alumina support against thermally induced surface area loss and increases the dispersion of noble metals (*4–7*).

One aspect of cerium that has received the most attention in the recent literature is its role as an "oxygen storage" component in influencing the dynamic behavior of three-way catalysts under cycled air-fuel ratio (A/F) conditions. Such a storage component would adsorb or react with excess oxygen during excursions to the lean (net-oxidizing) side of the stoichiometric point. During subsequent rich (net-reducing) excursions, the stored oxygen would then be available for reaction with the reducing agents, thereby enhancing the conversion of CO and hydrocarbons. Research topics in this area have included measurements of the capacity and rate of the oxygen storage/release (i.e., catalyst oxidation/reduction) process (*2, 8–11*), catalyst response to a step A/F change (*12, 13*), and catalyst performance in a cycled feed as a function of the amplitude and frequency of the A/F oscillations (*8, 14–17*).

In addition to enhancing the transient performance of three-way catalysts through the oxygen storage mechanism just described, cerium can alter the kinetic behavior of three-way catalysts as a result of its interaction with supported noble metals. Summers and Ausen (*18*) have observed that the steady-state CO oxidation activity of a Pt/Al_2O_3 catalyst is enhanced upon addition of small quantities of Ce (0.6 to 1.3 wt%). Further increases in the Ce content, however, were found to deteriorate the CO oxidation activity. A recent kinetic study

0021-9517/88 $3.00

with alumina-supported noble metal catalysts containing cerium (*19*) has shown that the presence of cerium oxides tends to suppress the usual CO inhibition effect during the CO oxidation and to lower its activation energy. However, relatively little is known about the mechanism by which cerium additives modify the CO oxidation kinetics over supported noble metal catalysts.

In this paper we have examined, in laboratory feedstreams, the CO oxidation activity of a series of alumina-supported Rh catalysts promoted with different levels of cerium in order to improve our understanding of the kinetic behavior of the Rh/Ce/Al_2O_3 catalyst stream. Our choice of CO oxidation as a probe reaction was prompted not only by its practical significance in automotive emission control but also by its well established reaction mechanism over Rh (*20*). As this paper will show, the latter aspect of CO oxidation is useful in making inferences from the kinetic data about the nature of Rh–Ce interactions and the catalyst surface structure.

EXPERIMENTAL

Catalysts

A series of Rh/Ce/Al_2O_3 catalysts of fixed Rh loading (0.014 wt%) and variable Ce loadings (0 to 15 wt%) was prepared by stepwise impregnation of Al_2O_3 spheres (3.5 mm diameter, 112 m^2/g BET surface area) to incipient wetness. For samples containing Ce, the Ce was deposited onto the support from $Ce(NO_3)_3$ aqueous solutions and then calcined in flowing air at 500°C for 4 h prior to Rh impregnation with an aqueous solution of $RhCl_3$. The same calcination step (4 h at 500°C in air) followed the latter impregnation. Electron microprobe measurements show that such procedures resulted in a shallow ($\leq$20 μm) Rh band near the pellet's outer edge and a uniform distribution of the Ce throughout the catalyst beads.

The additional characteristics of the catalysts are listed in Table 1. The X-ray diffraction (XRD) data of the Rh/Ce/Al_2O_3 catalysts identified CeO_2 as the major cerium species for Ce loadings $\geq$2 wt%. The failure to detect CeO_2 in the case of 1 wt% Ce appears to be related to the morphology of the cerium compound (e.g., formation of highly dispersed surface species) and not to an insufficient amount of Ce present in the sample, because an independent XRD analysis of a physical mixture of alumina and coarse CeO_2 powders having the same composition showed a distinct CeO_2 peak. The average CeO_2 particle sizes, obtained from Fourier analysis of the X-ray diffraction peaks (*21*), range from 28 to 65 Å in diameter and depend weakly on the Ce loading. The Rh dispersion of the Rh/Al_2O_3 catalyst was determined to be 29% from H_2 chemisorption measurements based on 1 : 1 stoichiometry between adsorbed hydrogen

TABLE 1

Characteristics of the 0.014 wt% Rh/Ce/Al_2O_3 Catalysts

Ce loading (wt%)	Compounds identified by XRD	CeO_2 particle diameter (Å)	BET surface area (m^2/g)	Rh dispersion (%)	Rh bandwidth[b] (μm)
0	Al_2O_3	—	112	29	18
1	Al_2O_3	—	NM[a]	NM[a]	NM[a]
2	Al_2O_3, CeO_2	28	109	25	20
9	Al_2O_3, CeO_2	53	NM[a]	NM[a]	11
15	Al_2O_3, CeO_2	65	87	NM[a]	NM[a]

[a] Not measured.

[b] Width at half-maximum height of electron microprobe traces.

atoms and surface Rh atoms. A similar Rh dispersion was measured for the Rh/Al_2O_3 catalyst containing 2 wt% Ce, indicating that the Rh particle size is little affected by the presence of cerium on the alumina support surface. (Ceria reducibility as measured by separate H_2 uptake experiments (*22*) was found to be virtually unaffected by the presence of small amounts of noble metals in the sample, and thus the reducible nature of the ceria additive would not interfere with the determination of Rh dispersions based on H_2 chemisorption measurements.) The BET surface area of the support, however, tends to decrease appreciably (from 112 to 87 m^2/g) as the Ce loading increases (from 0 to 15 wt%). This loss of surface area, presumably caused by plugging of some of the micropores of the alumina support (*18*), is expected to have minimal effects on the catalytic activity because the support surface area is still high enough to maintain the noble metal reasonably well dispersed.

To investigate the effects of impregnation sequence on the catalyst surface structure (and thus on the catalytic properties), additional $Rh/Ce/Al_2O_3$ catalysts were prepared by the reverse sequence of impregnations (i.e., deposition of Rh followed by Ce). The same Ce and Rh salts were used and the catalysts were calcined at 500°C for 4 h after each impregnation step. Electron microprobe analysis of the pellet's cross section again showed a shallow (~30 μm) surface band of Rh, with the Ce being uniformly distributed throughout the beads.

As a limiting case of the $Rh/Ce/Al_2O_3$ system described above, a 0.014 wt% Rh catalyst supported on pure CeO_2 was prepared by pelletizing ceria powder and then impregnating the ceria pellets with an aqueous solution of $RhCl_3$. The ceria powder was synthesized by spray drying an aqueous solution of cerium nitrate, citric acid, and nitric acid (*23*). (This spray-dried CeO_2 powder has a reasonably high BET surface area of 56 m^2/g, compared with less than 2 m^2/g BET area for commercial ceria powders.) Prior to pelletization the ceria powder was sintered at 800°C for 4 h in a muffle furnace and then ball milled overnight. The resulting powder was mixed with water containing 5% polyvinyl alcohol (PVA) and extruded through a stainless-steel tube to form cylindrical pellets approximately 5 mm long and 4 mm in diameter. These pellets were treated at 400°C to remove the H_2O and PVA and then heated in a temperature-programmed oven at 5°C/min to 950°C. Such procedures yielded pellets with adequate mechanical strength and a stable BET area of 20 m^2/g.

Mercury porosimetry data for the ceria pellet revealed a monomodal pore-size distribution (average pore diameter = ~350 Å) with a pore volume of 0.19 cm^3/g. This relatively small pore volume of the support made it necessary to employ an excess volume impregnation technique (rather than the conventional incipient wetness method) in order to minimize pellet-to-pellet variation in Rh deposition. In this technique, the adsorbate solution was obtained by dissolving the desired amount of $RhCl_3 \cdot 3H_2O$ in just enough H_2O to cover the top of the pellets, and the adsorption of the Rh precursor on the pellets was allowed to occur for $1\frac{1}{2}$ h while agitating them frequently. After impregnation the catalyst was calcined in the usual manner (500°C, 4 h, air) and such procedures resulted in the deposition of the Rh near the periphery of the CeO_2 pellets.

Characterization of CO Adsorption

Temperature-programmed desorption (TPD) and infrared (IR) spectroscopies were used to characterize the CO adsorption properties of Rh/Al_2O_3 catalysts with and without Ce. The apparatus and the sample preparation techniques for the TPD and IR experiments have been described previously (*24, 25*). TPD spectra were obtained using the powder samples ($\leq$1 mg) scraped off the surface metal band of the standard $Rh/Ce/Al_2O_3$ catalysts described above. After a CO dose at 0°C to the

saturation coverage, the catalyst sample was heated under vaccuum at a linear rate of 5°C/s while monitoring the partial pressures of desorbing gases using a mass spectrometer. IR spectra were taken in flowing CO using 0.48 wt% Rh/Al_2O_3 and 0.46 wt% Rh/10 wt% Ce/Al_2O_3 wafers each obtained by pressing approximately 100 mg of the impregnated powder into a 0.2-mm-thick, self-supporting disk. These Rh loadings were selected to approximate the local concentration of Rh in the shallow surface band of our 0.014 wt% Rh catalysts.

CO Oxidation Activity Measurements

The CO oxidation activity of the catalysts was measured in laboratory $CO–O_2$ feedstreams (in a N_2 background) using an internal-recycle mixed-flow reactor (*26*). This stainless-steel reactor contains a stationary catalyst basket, and the gases are mixed with a magnetically driven impeller. All the data reported here were obtained at an impeller speed of 1500 rpm and a space velocity of 32,000 h^{-1} (a total feedstream flow rate of 5 liters/min through 4.5 g of catalyst). Prior to each experiment, the catalyst sample was reduced for 30 min in 5 vol% H_2 at 450°C after a 15-min treatment in 2 vol% at the same temperature.

The catalyst activity was characterized in two ways: (i) temperature run-up experiments with fixed composition, and (ii) isothermal experiments with variable composition. Temperature run-up experiments involved monitoring steady-state reactor outlet concentrations of CO, O_2, and CO_2 as a function of temperature (increased from room temperature to 450°C) in a feedstream of fixed composition. The effects of CO and O_2 concentrations on the CO oxidation activity of the catalysts were examined by repeating the temperature run-up experiments over a range of feedstream compositions (0.3 to 6 vol% CO and 0.25 to 5 vol% O_2). In this study we arbitrarily chose the temperature required for 1000 ppm CO_2 production as a basis for comparison of the catalyst activities. We also conducted a series of temperature run-up experiments with constant *outlet* composition to determine the apparent activation energy. (Maintaining constant outlet composition in a CSTR such as our reactor ensures that the catalyst sample is exposed to a constant gaseous composition during temperature run-up, thus allowing one to extract the temperature dependence of the reaction rate from the experiment data.) Isothermal experiments, on the other hand, are convenient in examining how the reaction rate depends on the gas-phase concentration of the individual reactants. This information about the reaction order is useful because it often provides insight into the reaction mechanisms over the catalyst sample being studied.

RESULTS

Effects of Ce Addition on CO Adsorption

Figure 1 compares the TPD spectra of CO from the 0.014 wt% Rh/Al_2O_3 catalysts containing 0, 2, and 9 wt% Ce. Each spectrum in Fig. 1 is characterized by two distinct peaks: one around 50°C and the other at temperatures bewteen 225 and 240°C. The low-temperature peak is associated with CO weakly adsorbed onto the blank alumina support, as confirmed by a separate TPD experiment with Al_2O_3. (The CO TPD spectrum for Ce/Al_2O_3 was virtually the same as that for Al_2O_3, indicating

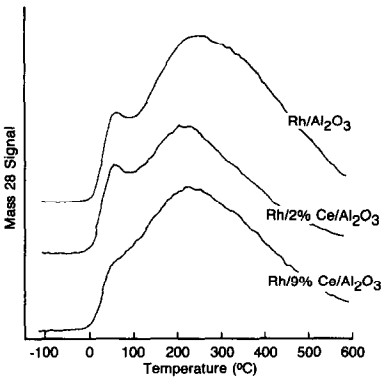

FIG. 1. TPD spectra (displaced vertically for clarity) of CO from 0.014 wt% Rh/Al_2O_3 with and without Ce. The samples were initially saturated with CO at 0°C.

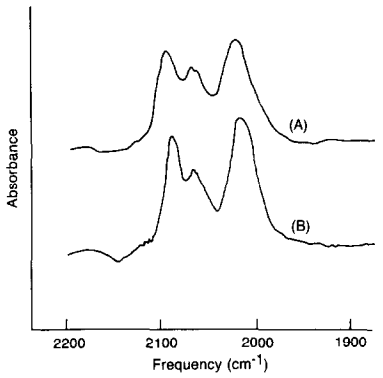

FIG. 2. IR spectra (displaced vertically for clarity) of CO adsorbed on (A) 0.48 wt% Rh/Al_2O_3 and (B) 0.46 wt% Rh/10 wt% Ce/Al_2O_3. The spectra were taken at 150°C in flowing CO.

little interaction between CO and Ce.) Although rather broad and poorly resolved, the TPD spectra at the high temperatures (associated with CO adsorbed on Rh) for the Ce-containing catalysts are similar to that for the Ce-free counterpart. This suggests that the CO adsorption characteristics on supported Rh are not significantly altered by the presence of cerium.

A similar conclusion was obtained from IR spectroscopic studies of CO adsorption on Rh/Al_2O_3 with and without Ce. As shown in Fig. 2, both the Rh/Al_2O_3 and the $Rh/Ce/Al_2O_3$ catalysts exhibit the well-established spectral features: linear-CO band at $\sim$2060 cm^{-1} and the dicarbonyl bands at 2085 and 2020 cm^{-1}. (The intensity of the band of bridge-bonded CO is usually low.) One important point to note is that the frequencies for both the dicarbonyl and the linear-CO species remained virtually unchanged upon Ce addition to the Rh/Al_2O_3 catalyst. This suggests the absence of appreciable electronic effects caused by the Ce additive, in agreement with our TPD results indicating that the adsorptiove property of CO on supported Rh is unaffected by the presence of Ce.

Effects of Ce Addition on Kinetics

The purpose of this section is to discuss how the kinetics of CO oxidation over Rh/Al_2O_3 are affected by the presence of Ce. Here we will focus on the behavior of the Rh/Al_2O_3 catalyst containing 9 wt% Ce; the effects of Ce loading will be discussed later in this paper.

Figure 3 compares the rates of CO oxidation measured over 0.014 wt% Rh/Al_2O_3 (closed circles) and 0.014 wt% Rh/Al_2O_3 containing 9 wt% Ce (open squares) at 196°C. In these experiments, the CO concentration was varied nearly three orders of magnitude (0.01 to 6 vol%) while holding the O_2 concentration constant at 0.5 vol%. In accord with results of earlier kinetic studies (*20, 27*), the rate data for the Rh/Al_2O_3 catalyst exhibits a transition from first order in CO to negative first order as the CO concentration is increased. The negative first-order dependence of the reaction rate on CO concentration (i.e., CO inhibition effect) observed at high CO concentrations is a direct consequence of the fact that the catalyst surface is predominantly covered with adsorbed CO, thereby blocking the adsorption of oxygen (*20*). It is interesting to note that in the regime of low CO concentrations both the Rh/Al_2O_3 and the $Rh/Ce/Al_2O_3$ catalysts show very similar reaction rates. In the high CO concentration regime, however, there is a drastic

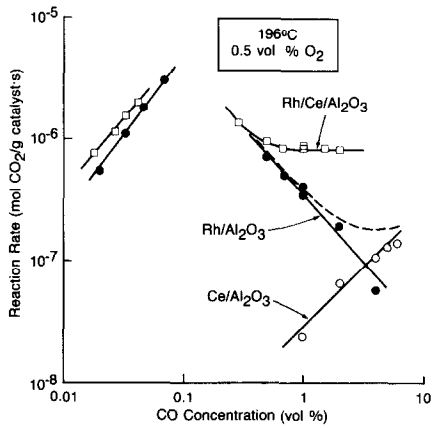

FIG. 3. CO oxidation rates over 0.014 wt% Rh/Al_2O_3 and 0.014 wt% Rh/9 wt% Ce/Al_2O_3 as a function of CO concentration. The dashed curve represents the rate over a physical mixture of Rh/Al_2O_3 and Ce/Al_2O_3.

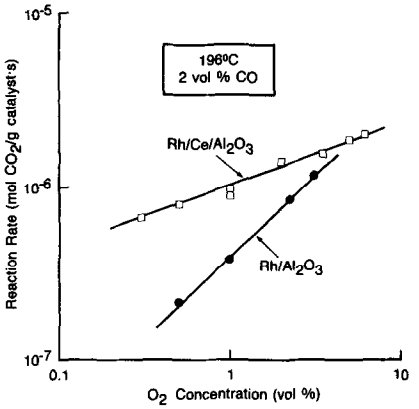

FIG. 4. CO oxidation rates over 0.014 wt% Rh/Al_2O_3 and 0.014 wt% Rh/9 wt% Ce/Al_2O_3 as a function of O_2 concentration.

difference in kinetic behavior between the two catalysts; in contrast to the Rh/Al_2O_3 catalyst (whose rate is inhibited by CO), the CO oxidation rate over the $Rh/Ce/Al_2O_3$ catalyst depends only weakly on CO concentration. This suppression of the CO inhibition effect over $Rh/Ce/Al_2O_3$ leads to a higher CO oxidation activity than its Ce-free counterpart for CO concentrations higher than 0.4 vol%.

It is important to emphasize that this enhanced CO oxidation activity observed over the $Rh/Ce/Al_2O_3$ catalyst at high CO concentrations is not due to the additional activity derived from the Ce. This becomes apparent when the reaction rates for a physical mixture of the Ce/Al_2O_3 and Rh/Al_2O_3 catalysts (dashed curve of Fig. 3) are compared with those for the $Rh/Ce/Al_2O_3$ catalyst. (The curve for the physical mixture was obtained by adding the measured rates over the 9 wt% Ce/Al_2O_3 and 0.014 wt% Rh/Al_2O_3 catalysts.) It can be seen that the $Rh/Ce/Al_2O_3$ catalyst is considerably more active than the physical mixture in the high CO concentration regime, despite the fact that both samples contain the same absolute amounts of Ce and Rh. This comparison clearly demonstrates that the coexistence of Rh and Ce in the same catalyst pellet provides a synergistic enhancement of CO oxidation activity.

Figure 4 shows that the kinetic behavior in the rate vs O_2 concentration domain is also altered significantly by the addition of cerium. For Rh/Al_2O_3 itself, the rate increases linearly with increasing O_2 concentration, as reported previously (*20*). The reaction over $Rh/Ce/Al_2O_3$, on the other hand, increases rather gradually upon increasing O_2 concentrations, exhibiting 0.37th reaction order in oxygen. Thus, the presence of Ce in the Rh/Al_2O_3 catalyst tends to decrease the sensitivity of the rate to gas-phase O_2 concentration.

Furthermore, the addition of cerium to the Rh/Al_2O_3 catalyst has a strong influence on the apparent activation energy for the reaction. As illustrated in Fig. 5, the CO oxidation over Rh/Al_2O_3 over the wide range of O_2/CO gas-phase concentration ratios (1 vol% CO, 0.5 to 5 vol% O_2) is characterized by relatively constant activation energies of 26 to 28 kcal/mol. These activation energy values are close to the desorption energy of CO from Rh surfaces and consistent with the generally accepted mechanism for CO oxidation where the reaction rate is controlled by the rate of creation of vacant sites as a result of CO desorption from the CO-saturated Rh surface (*20, 28*). Unlike the case of Rh/Al_2O_3, the apparent activation energy for the Ce-containing Rh/Al_2O_3 catalyst changes ap-

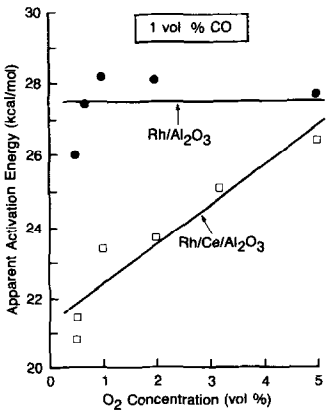

FIG. 5. Apparent activation energies for CO oxidation over 0.014 wt% Rh/Al_2O_3 and 0.014 wt% Rh/9 wt% Ce/Al_2O_3 as a function of O_2 concentration.

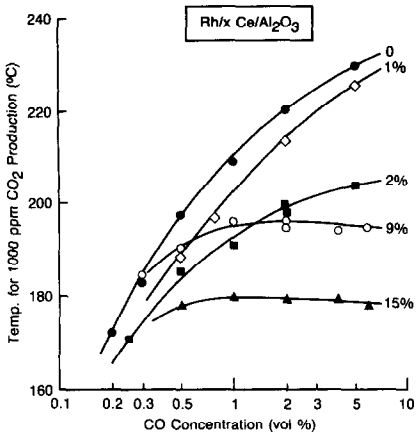

FIG. 6. Temperatures for 1000 ppm CO_2 production over 0.014 wt% Rh/Al_2O_3 containing variable levels of Ce as a function of the CO concentration in the feed. The feedstream concentration of O_2 was held constant at 0.5 vol%.

preciably in response to changes in the stoichiometry of the reactant mixture; the activation energy for $Rh/Ce/Al_2O_3$ was found to decrease from 26.5 to 21 kcal/mol as the O_2 concentration decreased from 5 to 0.5 vol%. It is interesting to note that in the strongly oxidizing environment (5 vol% O_2), similar apparent activation energies were observed for the Rh/Al_2O_3 catalysts with and without Ce.

Effects of Ce Loading

Recall that all the data discussed above were obtained with the Rh/Al_2O_3 catalyst containing 9 wt% Ce. We conducted a series of temperature run-up experiments to characterize the CO oxidation activity of the Rh/Al_2O_3 catalysts with Ce loadings ranging from 0 to 15 wt%. Figure 6 shows the results of such experiments in feedstreams containing 0.5 vol% O_2 and variable levels of CO (5 liters/min through 4.5 g of catalyst). The temperature required for 1000 ppm CO_2 production was taken as a convenient basis for comparison of CO oxidation activity. The observation that the temperature for 1000 ppm CO_2 production for Rh/Al_2O_3 increases monotonically with increasing CO concentration is not surprising in view of the strong CO inhibition effect on the CO oxidation rate illustrated in Fig. 3 and in our earlier study (*20*). The sample containing 1 wt% Ce (as well as the 0.5 wt% Ce case not shown in the figure) exhibits essentially the same CO concentration dependence of the oxidation activity. In the presence of 2 wt% Ce in the Rh/Al_2O_3 catalyst, however, the CO inhibition effect is suppressed significantly, as evidenced by the less steep rise of the curve with increasing CO concentration. The addition of 9 or 15 wt% Ce to the catalyst further suppresses the CO inhibition effect, so that the reaction rate becomes virtually independent of CO concentration over the range 0.5 to 6 vol% CO.

In addition to the suppression of the CO inhibition effect discussed above, increasing the Ce content in the Rh/Al_2O_3 catalyst tends to render its CO oxidation activity increasingly less sensitive to variations in the O_2 concentration. This aspect is illustrated in Fig. 7, where the temperature for 1000 ppm CO_2 production is plotted against O_2 concentration (CO concentration fixed at 2 vol%) for various Ce loadings. As can be anticipated from the first-order oxygen dependence of the CO oxidation rate over

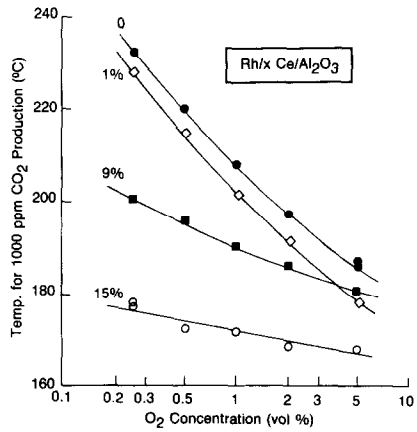

FIG. 7. Temperatures for 1000 ppm CO_2 production over 0.014 wt% Rh/Al_2O_3 containing variable levels of Ce as a function of the O_2 concentration in the feed. The feedstream concentration of CO was held constant at 2 vol%.

TABLE 2

Apparent Activation Energy for the CO Oxidation as a Function of Ce Loading

Ce loading (wt%)	Activation energy (kcal/mol)
0	28.2
1	26.7
9	23.4
15	20.3

Rh/Al_2O_3 [Fig. 4 and Ref. (*20*)], the temperature required for 1000 ppm CO_2 production for the Ce-free catalyst sample decreases markedly with increasing O_2 concentration. As was also the case in Fig. 6, such a kinetic behavior characteristic of the Ce-free Rh/Al_2O_3 catalyst is not altered by the addition of 1 wt% Ce. Note, however, that further increases in the Ce content (see the curves for 9 and 15 wt% Ce) enhance the CO oxidation activity and reduce its sensitivity to O_2 concentration.

We also measured the apparent activation energy for the CO oxidation as a function of the Ce loading in the Rh/Al_2O_3 catalysts. Table 2 shows the activation energy values determined in a reactant stream containing 1 vol% CO and 1 vol% O_2. It can be seen that the activation energy decreases from 28.2 to 20.3 kcal/mol as the Ce loading is increased from 0 to 15 wt%.

Effects of Impregnation Sequence

Recall that the standard catalysts examined so far were prepared by depositing Rh onto the Ce-impregnated Al_2O_3 support. To assess the importance of impregnation sequence, some additional temperature run-up experiments were conducted with $Rh/Ce/Al_2O_3$ catalysts prepared by the reverse sequence of impregnations (i.e., Rh impregnation followed by Ce impregnation). Comparisons are made in Fig. 8 between the cases of the standard (solid lines) and reverse (dashed lines) impregnation sequences for two different Ce loadings. Although different impregnation sequences resulted in somewhat different activity levels, there are close similarities in the dependence of the reaction rate on CO concentration for the samples containing both 0.5 and 15 wt% Ce. It is evident from Fig. 8 that the kinetic behavior of the $Rh/Ce/Al_2O_3$ catalysts during CO oxidation depends primarily on the amount of Ce additives and not on the order of Ce and Rh impregnations. These observations are useful in making inferences about the distribution of the Ce and Rh on the Al_2O_3 support surface, as will be discussed later.

DISCUSSION

The results of the present study show that the extent to which the Ce additive affects the CO oxidation kinetics depends strongly on the stoichiometry of the reactant mixture. In the presence of a large excess of oxygen over CO (see Fig. 3; <0.1 vol% CO), for example, the reaction kinetics are not significantly affected by the presence of Ce in the Rh/Al_2O_3 catalysts. In this strongly oxidizing environment, the alumina-supported Rh surface would be populated with relatively high concentrations of adsorbed oxygen atoms and low concentrations of adsorbed CO (*29*). A sim-

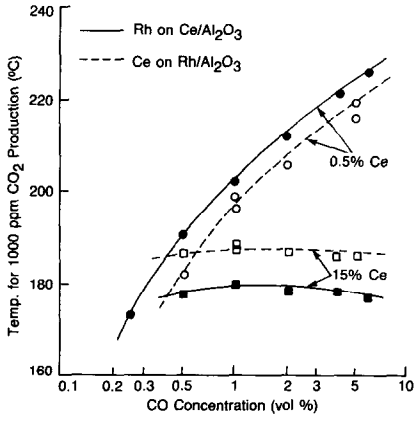

FIG. 8. Temperatures for 1000 ppm CO_2 production over $Rh/Ce/Al_2O_3$ catalysts prepared by two different impregnation sequences (solid curves, standard; dashed curves, reverse). The feedstream concentration of O_2 was held constant at 0.5 vol%.

ilar distribution of these two adsorbates on the metal surface is expected for the $Rh/Ce/Al_2O_3$ catalysts, because our IR and TPD spectra (see Figs. 1 and 2) indicate that the CO adsorption characteristics on Rh are not altered appreciably by the presence of Ce. In this case, the limited amount of adsobed CO on the Rh surface would be rapidly consumed via reaction with the adsorbed oxygen atoms (rather than via reaction with less reactive surface lattice oxygen derived from the cerium oxides). Thus, it is reasonable to assume that in a strongly oxidizing environment, the primary pathway for CO oxidation over Rh/Al_2O_3 with or without Ce is the usual Langmuir–Hinshelwood reaction occurring on the Rh surface between adsorbed CO and adsorbed oxygen. This argument is consistent with the observations that the Rh/Al_2O_3 and $Rh/Ce/Al_2O_3$ catalysts exhibit close similarities in both the CO oxidation rates (and their dependence on CO concentration) and the apparent activation energies in the strongly oxidizing regimes (i.e., high O_2/CO concentration ratios) of Figs. 3 and 5. We believe that the formation of Rh oxides is unlikely to be a factor in interpreting the kinetic data in these strongly oxidizing regimes (O_2/CO ratio <25); a previous surface study conducted on a Rh field emitter tip at a comparable temperature (500 K) detected no significant Rh oxide formation until the O_2/CO gas-phase concentration ratio reached 40 (*30*).

Under net-reducing or moderately oxidizing conditions (see Fig. 3; >0.5 vol% CO), on the other hand, the kinetics of CO oxidation are altered appreciably by the presence of cerium additives. Under these conditions the CO oxidation rate over the Ce-free Rh/Al_2O_3 catalyst decreases with increasing gas-phase CO concentration as a result of limited oxygen adsorption onto the catalyst surface nearly saturated with adsorbed CO (*20*). However, this CO inhibition effect resulting from a deficiency of surface oxygen was not observed over the Ce-containing Rh/Al_2O_3 catalysts. In view of the well-known oxygen storage/release property of ceria, we propose that the CO oxidation rate over the $Rh/Ce/Al_2O_3$ catalysts under net-reducing or moderately oxidizing conditions is enhanced by another pathway involving a surface reaction between CO adsorbed on Rh and oxygen derived from ceria. (Our TPD and IR studies show that the criteria supported on Al_2O_3 has a minimal interaction with CO.) This additional oxygen from the ceria would make the surface concentration of oxygen in the presence of Ce higher than that in the absence of Ce. Thus, a suppression of the CO inhibition effect and decreased sensitivity of the rate to gas-phase O_2 concentration would be expected for $Rh/Ce/Al_2O_3$, as observed in Figs. 3 and 5.

Kinetic evidence for the direct participation of lattice oxygen derived from ceria in the CO oxidation was obtained by measurements of CO oxidation rates over Rh/15 wt% Ce/Al_2O_3 and Rh/CeO_2 as a function of CO concentration. The results of such experiments at 180°C are shown in Fig. 9. (The arrows in the low CO concentration regime represent rate oscillations observed for Rh/15 wt% Ce/Al_2O_3.) The close similarity in the kinetic behavior of the two catalysts is a strong indication that the nature of the Rh–Ce interaction in the $Rh/Ce/Al_2O_3$ system may be the same as that in the CeO_2-supported Rh catalyst. In

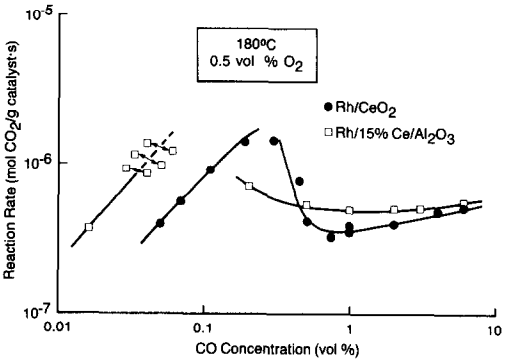

FIG. 9. Comparison of the CO oxidation rates over 0.014 wt% Rh/15 wt% Ce/Al_2O_3 and 0.014 wt% Rh/CeO_2.

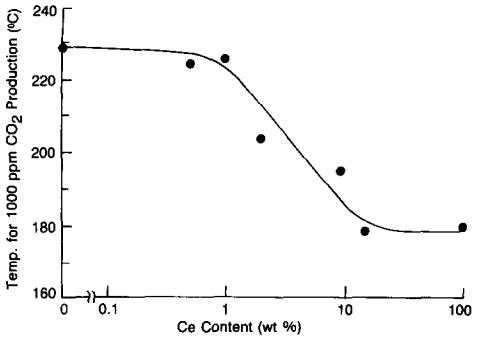

FIG. 10. Effect of the Ce content in the 0.014 wt% Rh/Al_2O_3 catalysts on the temperature for 1000 ppm CO_2 production in a feedstream containing 5 vol% CO and 0.5 vol% O_2.

the case of CeO_2-supported Pt catalysts where all the metal particles are in direct contact with CeO_2, lattice oxygen at the Pt/ceria interface has been shown to be responsible for the formation of CO_2 during CO TPD (*31*). Interface lattice oxygen is expected to play a similar role during CO oxidation over Rh/CeO_2.

The key feature of the reaction mechanism proposed above for the $Rh/Ce/Al_2O_3$ system is the interaction between Rh (acting as a CO source) and ceria (acting as an oxygen source) to form CO_2. While the Rh–CeO_2 intimacy requirement for their interaction cannot be determined from our experiments, a combination of the XRD data (Table 1) and the kinetic data (Figs. 6 and 7) suggests that three-dimensional CeO_2 particles present in our high-cerium samples ($\geq$2 wt% Ce) are more effective in donating oxygen than highly dispersed ceria formed on the alumina surface at low Ce loadings ($\leq$1 wt% Ce). This is reasonable in view of recent XPS studies of alumina-supported ceria (*32, 33*), which show that Ce at low loadings tends to form a ceria–alumina surface species exhibiting a Ce^{3+}-like feature (i.e., oxygen-deficient) as a result of its strong interaction with alumina.

The effects of Ce loading on the CO oxidation activity can be rationalized on the basis of the above mechanism. Figure 10 shows how the temperature required for 1000 ppm CO_2 production changes with the Ce content in the Rh/Al_2O_3 catalyst for a reactant mixture containing 5 vol% CO and 0.5 vol% O_2 (activity data taken from Fig. 6, except for the 100% Ce case). In this strongly reducing feedstream where the proposed reaction mechanism would dominate, addition of 2 wt% Ce or more was found to enhance the CO oxidation activity, as evidenced by the decrease in the temperature for 1000 ppm CO_2 production. This can be attributed to the fact that as the Ce loading is increased, the number of CeO_2 particles in the vicinity of the Rh particles would increase, thereby increasing the availability of the surface oxygen for CO oxidation. (The size of the CeO_2 particles does not appear to be a factor here because, as Table 1 shows, the average CeO_2 particle size changes relatively little over the Ce loading range of 2 to 15 wt%.) The observation that the CO oxidation activity of Rh/15 wt% Ce/Al_2O_3 is comparable to that of Rh/CeO_2 (i.e., 100% Ce case) is not surprising, because the rate of oxygen supply (and thus the reaction rate) at sufficiently high Ce loadings would be expected to be limited by the circumference of the Rh particles.

Another possible mode of Rh–Ce interaction in the CO oxidation might be the decoration of the Rh particles by partially reduced cerium oxide moieties. It is conceivable that our $Rh/Ce/Al_2O_3$ catalysts might have been in such an SMSI (strong metal–support interaction) state during the activity measurements, because our catalyst samples were reduced at 450°C prior to each experiment. During the high-temperature reduction step, portions of rare earth oxide additives (e.g., CeO_2) in contact with the metal particles can undergo partial reduction, resulting in the migration of the rare earth oxide patches onto the metal surface (*34*). However, we rule out this possibility for the following reasons.

First, as shown in Fig. 11, H_2 chemisorp-

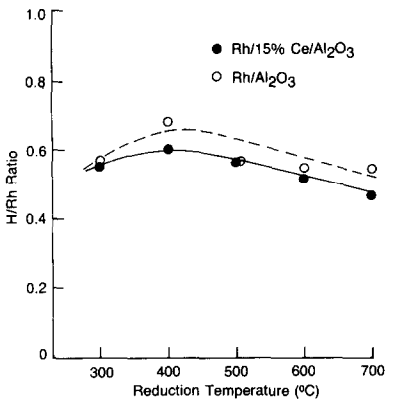

FIG. 11. H_2 uptake of 0.2 wt% Rh/Al_2O_3 with and without Ce after reduction treatment (4 h in H_2) at varying temperatures.

tion measurements with a 0.2 wt% Rh/Al_2O_3 catalyst containing 15 wt% Ce showed no drastic suppression of H_2 uptake even after high-temperature reduction. (This higher Rh loading than that of our standard $Rh/Ce/Al_2O_3$ catalysts was chosen for more reliable chemisorption measurements.) The small decrease in the H/Rh ratio at reduction temperatures higher than 400°C is presumably related to the usual sintering of the Rh particles (rather than SMSI induced by the Ce additive), as evidenced by the similar trend observed with Rh/Al_2O_3. The second argument against SMSI is based on the recent observations (*35, 36*) that the SMSI state can largely be reversed even upon room-temperature exposure to O_2. Since all the activity measurements reported here were done above 170°C in the presence of significant amounts of O_2, Rh–Ce interactions through SMSI are not likely to have affected the CO oxidation kinetics in our case. Finally, we observed a close similarity in the reaction rates between Rh/Al_2O_3 and $Rh/Ce/Al_2O_3$ in the low CO concentration regime of Fig. 3. This also tends to argue against the SMSI hypothesis, because contrary to our observation, the attendant site blocking caused by a partial coverage of the Rh surface by cerium oxide moieties would presumably give substantially lower CO oxidation activity over $Rh/Ce/Al_2O_3$ under the strongly oxidizing conditions.

The results of Figs. 8 and 9 allow us to make some inferences about the distribution of Rh and Ce on the catalyst surface. As shown in Fig. 9, the addition of large amounts of Ce relative to Rh (≥2 wt% Ce vs 0.014 wt% Rh) is required for the onset of enhancement of CO oxidation activity over the standard $Rh/Ce/Al_2O_3$ catalysts prepared by a two-step impregnation procedure involving deposition of Ce followed by Rh. Furthermore, the activity of $Rh/Ce/Al_2O_3$ catalysts was found to increase rather gradually with increasing Ce content. These observations suggest that there occurred no preferential deposition of Rh on top of or along the perimeter of the cerium oxide particles during the Rh impregnation onto the CeO_2-modified Al_2O_3 support, presumably due to similar affinities of the noble metal complex for both Al_2O_3 and CeO_2. (This argument of similar affinities for oxides is inferred from the observation that noble metal impregnation profiles were not significantly affected by the presence of a wide variety of base metal oxide additives on alumina supports (*37*).) Similar nonselective deposition of cerium onto Rh-impregnated Al_2O_3 is expected to occur during the reverse impregnation, because the Rh would exist as oxides (primarily Rh_2O_3) on the alumina support after its impregnation and subsequent calcination (*38*). This is further supported by the observation of the insensitivity of the reaction kinetics to the sequence of impregnations (see Fig. 8). From these considerations, it is reasonable to hypothesize that most of the added Ce interacts directly with the alumina support rather than with the Rh crystallites.

CONCLUDING REMARKS

Our laboratory reactor experiments with a series of $Rh/Ce/Al_2O_3$ catalysts have shown that the addition of cerium to a low-loaded Rh/Al_2O_3 catalyst results in modifications of the kinetics of CO oxida-

tion under moderately oxidizing or net-reducing conditions. The observed changes in the kinetics include a suppression of the CO inhibition effect, decreased sensitivity of the rate to O_2 concentration, and decreased apparent activation energy. Results of IR and TPD studies of CO adsorption on the $Rh/Ce/Al_2O_3$ catalysts tend to argue against charge transfer between the Rh and the Ce (and the resulting changes in the adsorptive properties of Rh) as an explanation for the modifications of the CO oxidation kinetics in the presence of Ce. The effects of Ce addition on the CO oxidation kinetics observed here are best explained on the basis of a mechanism involving CO_2 formation via a surface reaction between CO adsorbed on Rh and lattice oxygen derived from the neighboring ceria particles. It was also observed that Ce addition affected the CO oxidation kinetics over Rh/Al_2O_3 in the same manner, regardless of whether the Ce was deposited before or after the Rh impregnation.

As a result of the Ce-induced kinetic modifications mentioned above, the $Rh/Ce/Al_2O_3$ catalysts exhibit substantially higher CO oxidation activity than the Ce-free counterpart in moderately oxidizing or net-reducing laboratory feedstreams. A similar enhancement of CO oxidation activity has been observed in engine exhaust when cerium was added to three-way catalysts (*39*).

ACKNOWLEDGMENTS

The authors thank M. J. D'Aniello and M. G. Zammit (chemisorption data), D. D. Beck and C. J. Carr (TPD spectra), R. A. Dictor (IR spectra), and B. R. Powell and R. L. Bloink (ceria powder synthesis and X-ray diffraction analysis) of the Physical Chemistry Department.

REFERENCES

1. Gandhi, H. S., Piken, A. G., Shelef, M., and Delosh, R. G., SAE Paper No. 760201, 1976.
2. Schlatter, J. C., and Mitchell, P. J., *Ind. Eng. Chem. Prod. Res. Dev.* **19,** 288 (1980).
3. Herz, R. K., and Sell, J. A., *J. Catal.* **94,** 166 (1985).
4. Hindin, S. G., Engelhard Mineral and Chemical Co., U.S. Patent 3,870,455 (1973).
5. Maselli, J., Ernest, M., and Graham, J., W. R. Grace Co., German Patent 2,362,601 (1974).
6. Kummer, J. T., Yao, Y., and McKee, D., SAE Paper No. 760143, 1976.
7. Yu Yao, Y.-F., Paper presented at "6th N. Amer. Catal. Soc. Mtg., Chicago, IL, March 1979."
8. Gandhi, H. S., Piken, A., Stepien, H., Shelef, M., Delosh, R., and Heyde, M., SAE Paper No. 770196, 1977.
9. Kaneko, Y., Kobayashi, H., Komagome, R., Hirako, H., and Nakayama, O., SAE Paper No. 780607, 1978.
10. Herz, R. K., *Ind. Eng. Chem. Prod. Res. Dev.* **20,** 451 (1981).
11. Su, E. C., Montreuil, C. N., and Rothschild, W. G., *Appl. Catal.* **17,** 75 (1985).
12. Sell, J. A., Herz, R. K., and Monroe, D. R., SAE Paper No. 800463, 1980.
13. Schulman, M. A., Hamburg, D. R., and Throop, M. J., SAE Paper No. 820276, 1982.
14. Schlatter, J. C., Sinkevitch, R. M., and Mitchell, P. J., *Ind. Eng. Chem. Prod. Res. Dev.* **22,** 51 (1983).
15. Falk, C. D., and Mooney, J. J., SAE Paper No. 800462, 1980.
16. Herz, R. K., Kiela, J., and Sell, J. A., *Ind. Eng. Chem. Prod. Res. Dev.* **22,** 381 (1983).
17. Taylor, K. C., and Sinkevitch, R. M., *Ind. Eng. Chem. Prod. Res. Dev.* **22,** 45 (1983).
18. Summers, J. C., and Ausen, S. A., *J. Catal.* **58,** 131 (1979).
19. Yu Yao, Y.-F., *J. Catal.* **87,** 152 (1984).
20. Oh, S. H., Fisher, G. B., Carpenter, J. E., and Goodman, D. W., *J. Catal.* **100,** 360 (1986).
21. Nandi, R. K., Kuo, H. K., Schlosberg, W., Wissler, G., Cohen, J. B., and Crist, B., *J. Appl. Crystallogr.* **17,** 22 (1984).
22. D'Aniello, M. J., Jr., unpublished results, General Motors Research Laboratories, Warren, MI (1987).
23. Powell, B. R., Bloink, R. L., and Eickel, C. C., *J. Amer. Ceram. Soc.* **71,** C–104 (1988).
24. Dictor, R. A., *J. Catal.* **109,** 89 (1988).
25. Beck, D. D., and Carr, C. J., *J. Catal.* **110,** 285 (1988).
26. Berty, J. M., *Chem. Eng. Prog.* **70,** 78 (1974).
27. Cant, N. W., Hicks, P. C., and Lennon, B. S., *J. Catal.* **54,** 372 (1978).
28. Goodman, D. W., and Peden, C. H. F., *J. Phys. Chem.* **90,** 4839 (1986).
29. Herz, R. K., and Marin, S. P., *J. Catal.* **65,** 281 (1980).
30. Kellogg, G. L., *J. Catal.* **92,** 167 (1985).
31. Jin, T., Okuhara, T., Mains, G. J., and White, J. M., *J. Phys. Chem.* **91,** 3310 (1987).
32. Le Normand, F., Bernhardt, P., Hilaire, L., Kili, K., Krill, G., and Maire, G., *Stud. Surf. Sci. Catal.* **30,** 221 (1987).

33. Shyu, J. Z., and Gandhi, H. S., Paper presented at the "10th N. Amer. Catal. Soc. Mtg., San Diego, CA, May 1987."
34. Rieck, J. S., and Bell, A. T., *J. Catal.* **99,** 278 (1986).
35. Anderson, J. B. F., and Burch, R., *Appl. Catal.* **25,** 173 (1986).
36. Herrmann, J. M., Gravelle-Rumeau-Maillot, M., and Gravelle, P. C., *J. Catal.* **104,** 136 (1987).
37. D'Aniello, M. J., Jr., U.S. Patent 4,380,510 (April 19, 1983).
38. Oh, S. H., and Carpenter, J. E., *J. Catal.* **80,** 472 (1983).
39. Schubert, P. J., Engler, B. H., and Koberstein, E., "The Influence of the Module Cerium Oxide/Alumina on Three-Way Catalyst Activity." Paper presented at the "61st ACS Mtg., Ann Arbor, MI, June 1987."